(Received 16 April 2025, Accepted 26 May 2025, Scheduled 4 June 2025)

A Miniaturized Ultra-Wideband Ground Penetrating Radar Antenna Based on the Vivaldi Structure

Zhiyao Qin[1], Shunfeng Cao[3], Weiheng Li[1], and Qiulin Huang[2, 3, *]

[1] *Hangzhou Institute of Technology, Xidian University, Hangzhou 310000, China*
[2] *National Key Laboratory of Radar Detection and Sensing, Xidian University, Xi'an 710071, China*
[3] *National Key Laboratory of Air-based Information Perception and Fusion, Luoyang 471099, China*

ABSTRACT: To meet the demands for a broader bandwidth, lower frequency, and enhanced gain, this article presents an innovative ultra-wideband miniaturized ground penetrating radar antenna based on traditional Vivaldi designs. The proposed antenna achieves an operational bandwidth spanning from 100 MHz to 2000 MHz (20 : 1 bandwidth ratio), with a peak gain reaching up to 9 dBi. Furthermore, it exhibits remarkable miniaturization. The antenna introduces novel dual-slotline configurations, side elliptical slots, metallic loading, and top-mounted lumped resistors, which collectively optimize its bandwidth and voltage standing wave ratio. These improvements make it particularly suitable for ground penetrating radar systems.

1. INTRODUCTION

Ground-penetrating radar (GPR) represents a significant breakthrough in non-destructive testing technology, offering the unprecedented possibility to acquire subsurface information without disturbing surface structures. This capability holds profound implications for various applications. In GPR systems, antennas play a pivotal role as the core component responsible for the transmission and reception of electromagnetic waves, directly influencing critical performance metrics such as detection accuracy and depth.

Within GPR technology, shorter wavelength electromagnetic waves can provide finer resolution results but are limited in their penetration depth through underground media. Conversely, longer wavelength waves enable deeper exploration into subsurface layers at the expense of reduced target resolution. Consequently, ultra-wideband (UWB) antennas offer a balanced approach to achieving both depth and precision in detection. Moreover, to enhance portability, it is generally desirable for GPR antennas to be compact in size.

Common UWB antennas include log-periodic antennas [1], helical antennas [2], and conical antennas [3]; however, these designs suffer from size constraints that hinder portability. Furthermore, horn antennas [4–8] and dipole antennas [9, 10] can also achieve UWB operation, and yet dipole antennas typically exhibit insufficient gain, which is crucial for determining detection depth in GPR applications.

Vivaldi antenna [11, 12], classified as a slot antenna, stands out for its advantages of high gain, wide bandwidth, and simple structure, making it an ideal candidate for GPR systems due to its ability to achieve UWB and high gain. Nevertheless, limitations in lower frequency performance necessitate modifications to meet the requirement for lower frequency emissions in GPR.

The Vivaldi antenna reported in [13] demonstrates ultra-wideband characteristics by employing dual slotlines, and yet the operating frequency remains inadequately low. As demonstrated by [14], a fractal-based antipodal Vivaldi antenna achieves ultra-wideband operation (4.2–42 GHz) through the integration of Koch fractal parasitic and dielectric lenses, significantly improving bandwidth, gain, and end-fire radiation compared to conventional designs. The proposed antenna, with dimensions of $186 \times 66 \times 1.524\,\text{mm}^3$, shows excellent agreement between simulation and measurement. However, the frequency is not low enough for ground-penetrating radar (GPR). To address this need, this article designs an ultra-wideband miniaturized antenna based on a Vivaldi antenna. By incorporating dual-slotlines, edge slotting, and metallic loading, this proposed antenna achieves an operational bandwidth spanning from 100 MHz to 2000 MHz, with a standing wave ratio predominantly below 3 across this range. It also demonstrates favorable radiation directionality, reaching a peak gain of 9 dBi, all while fulfilling the criteria for miniaturization.

2. ANTENNA CONFIGURATION

Based on the scaling principle of Vivaldi antennas, this work improves the conventional design to enhance radiation performance over a broader bandwidth while achieving miniaturization, as illustrated in Fig. 1. Key modifications include replacing the single-slotline with a dual-slot configuration to broaden bandwidth, etching side slots to optimize current distribution and reduce voltage standing wave ratio (VSWR), and applying metal loading on the top and side surfaces to lower the low-frequency cutoff for miniaturization. Additionally, lumped resistors are inserted between the radiating structure and top metal loading to suppress VSWR.

* Corresponding author: Qiulin Huang (qiulhuang@mail.xidian.edu.cn).

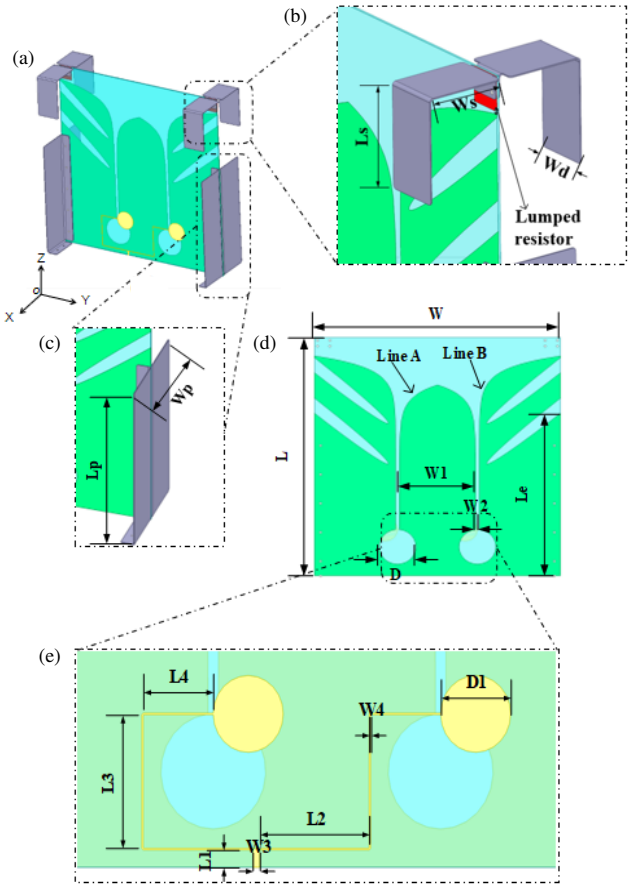

FIGURE 1. Configuration of the proposed antenna: (a) 3-D view, (b) top metal loading and lumped resistor, (c) side metal loading, (d) radiation structure, (e) feed structure.

The antenna is fabricated on a 2 mm-thick FR4 substrate ($\varepsilon_r = 4.4$, $\tan\delta = 0.02$). The design is supplemented by additional parametric specifications listed in Table 1. Full-wave electromagnetic simulations are executed using CST Studio Suite.

TABLE 1. Dimensions of the proposed antenna.

Par.	Value (mm)	Par.	Value (mm)
L	412	W	400
Lp	250	Ws	74
Ls	90	Wd	50
Le	281	Wp	150
$L1$	9.14	$W1$	124
$L2$	64.57	$W2$	6
$L3$	69.57	$W3$	3.9
$L4$	40	$W4$	0.86
D	60	$D1$	40

3. ANTENNA DESIGN AND ANALYSIS

3.1. Design of Slotline and Side-Slotting

The dual-slot structure employs two exponentially tapered curves with distinct parameters to independently adjust geometric characteristics of inner and outer slotlines. The inner slotline utilizes a smaller curvature parameter to enhance high-frequency radiation efficiency, while the outer slotline adopts a larger curvature design to improve low-frequency performance. Through systematic optimization of slot widths and curvature parameters, effective impedance matching and radiation capabilities are achieved across distinct frequency bands. This configuration significantly broadens the antenna's operational bandwidth while compensating radiation characteristics through complementary interactions between dual slots. After defining the exponential function-based slotlines, parameter tuning considers both antenna width and height. Final electromagnetic simulations enable precise adjustment of slot geometry and curvature parameters, yielding the optimized exponential function specifications for both slotlines as follows:

$$y_a = 0.000007837e^{0.05547x}, \quad (1)$$

$$y_b = 0.00004324e^{0.05668x}. \quad (2)$$

Elliptical slots inclined at 55° were incorporated on the radiator's side surfaces, with major and minor axes measuring 150 mm and 10 mm, respectively. This structural modification alters current distribution patterns, thereby achieving optimized VSWR characteristics.

Electromagnetic simulations of the antenna structure were conducted using Computer Simulation Technology (CST) software, with results illustrated in Fig. 2. Analysis of the electric field distribution patterns reveals the following: At lower frequencies, the longer electromagnetic wavelength causes concentrated radiation paths within the broader outer slotline region, where currents efficiently emit energy through this area. At higher frequencies, the significantly reduced wavelength enables energy radiation primarily through the narrower radiation aperture generated between the inner and outer slotlines. This design achieves robust radiation performance across a wide bandwidth while adapting to distinct electromagnetic wave propagation characteristics at different frequencies.

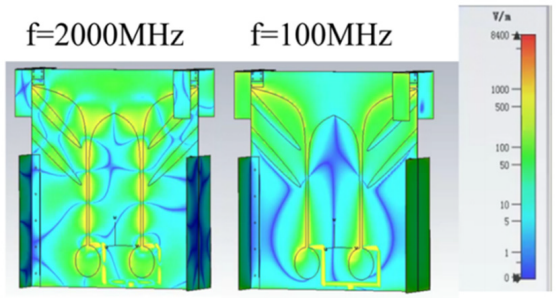

FIGURE 2. Electric field distribution comparison between 100 MHz and 2000 MHz (The figure shows the CST simulation results).

3.2. Design of Feed Structure

This study introduces an innovative feeding system improvement based on traditional Vivaldi antenna design principles. Conventional Vivaldi antennas typically employ direct microstrip-to-slotline transitions for feeding, achieving impedance matching and directional radiation through

tapered slot widths. However, this configuration demonstrates limitations in multi-slot structures, including uneven power distribution and impedance matching challenges.

To address the requirements of dual-slot Vivaldi antennas, our modified feeding architecture incorporates two critical enhancements. First, a Y-junction power divider converts the input 50 Ω impedance into two 100 Ω output ports, ensuring both balanced power distribution and synchronized excitation of dual slots. Second, a circular radiating patch functions as the impedance adaptation component, effectively bridging the power divider and conventional slotline structure. Precise diameter adjustment of this circular element enables effective matching to the 100 Ω impedance while maintaining radiation efficiency.

Electromagnetic simulations were conducted in CST Studio Suite to evaluate the antenna configuration with the parametric optimization of circular patch dimensions. As shown in Fig. 3, the structure achieves optimal broadband impedance matching when the patch diameter $D1$ is set to 40 mm.

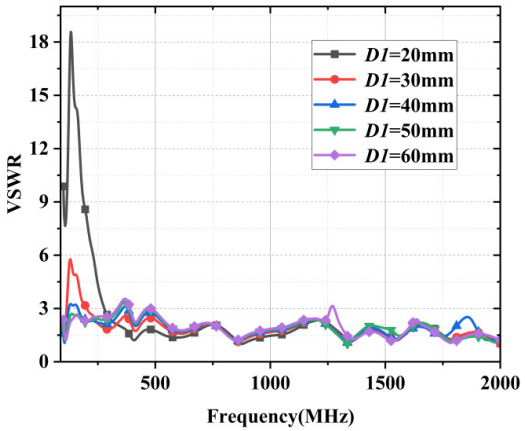

FIGURE 3. The VSWR for different circular patch diameters.

3.3. Design of Metal Loading

The operational bandwidth of the antenna was broadened by implementing metal loading structures on both the side and top surfaces, with the design evolution illustrated in Fig. 4. Building upon Ant I, Ant II introduced side-mounted metallic components, while subsequent modifications to Ant II incorporated a top-mounted radiating patch. Electromagnetic simulations revealed that extending the radiating patch length enhanced impedance matching, though excessive length increased antenna footprint. To address this trade-off, a novel meandered metal loading structure was developed in Ant III, effectively extending the electrical length of the radiating patch without physical size expansion. The final configuration (Ant III) integrates this meandered metal component with the radiating patch. The simulated VSWR results of the three antennas are illustrated in Fig. 5. As demonstrated by the simulation data, the impedance matching performance progressively improves with each structural modification of the antennas. Ultimately, all three antennas achieve excellent matching characteristics with VSWR values below 3 across the operational bandwidth.

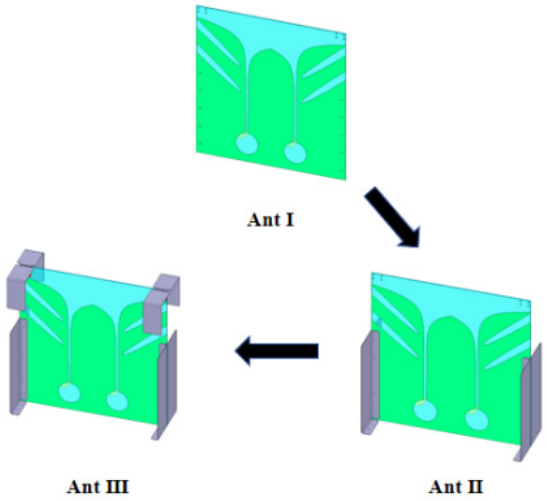

FIGURE 4. Evolution of metal loading.

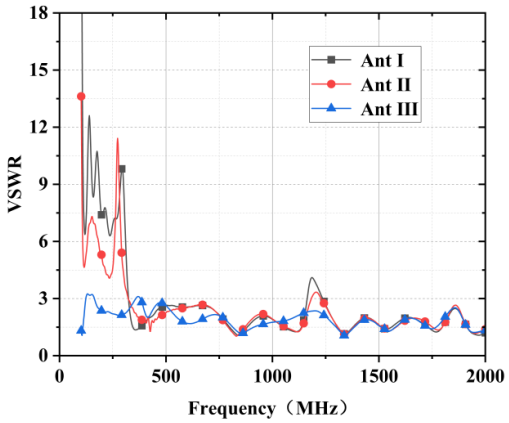

FIGURE 5. The VSWR for reference antennas and the proposed antenna.

TABLE 2. Comparisons between this work and previous research.

Ref.	Size (λ_L^3)	BW (GHz)	Gain (dBi)
[7]	0.188 × 0.145 × 0.08	0.87–4.5	3–9
[8]	0.387 × 4 × 1.24	1–30	6.7–19.4
[9]	0.16 × 0.08 × 0.03	0.18–2	−12–4.7
[10]	0.5 × 0.32 × 0.23	1.4–3.5	2.8–6
[11]	0.42 × 0.616 × 0.002	0.43–7	0–12
[12]	0.667 × 0.56 × 0.004	0.7–2.1	5–9
[13]	0.9 × 0.36 × 0.36	1.85–18.5	4–11.3
Pro.	0.137 × 0.133 × 0.05	0.1–2	−4–9

Note: λ_L is the free space wavelength at the lowest operational frequency.

3.4. Selection of the Lumped Resistance Value

The antenna structure was simulated using CST electromagnetic simulation software, and the lumped resistor value R was adjusted, as shown in Fig. 6. The results indicate that the match-

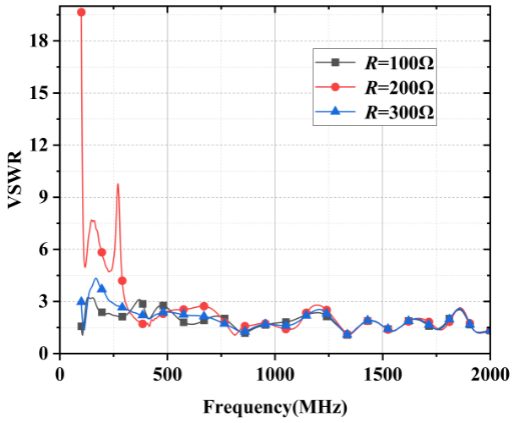

FIGURE 6. The VSWR for different values of the lumped resistor.

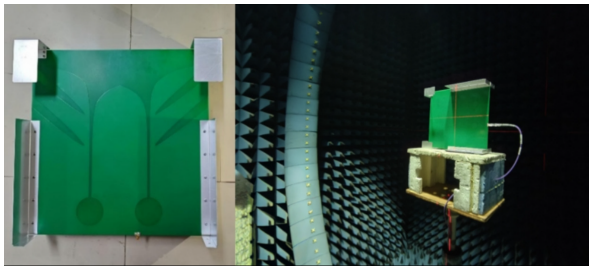

FIGURE 7. Photograph of the fabricated antenna and measured environment.

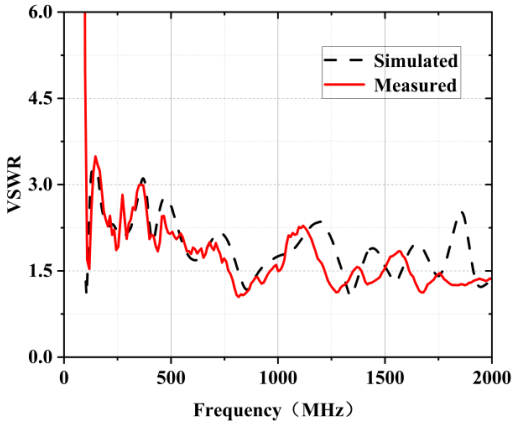

FIGURE 8. Measured and simulated VSWRs.

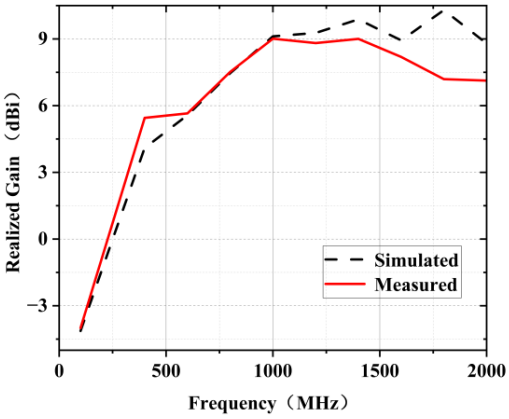

FIGURE 9. Measured and simulated gain.

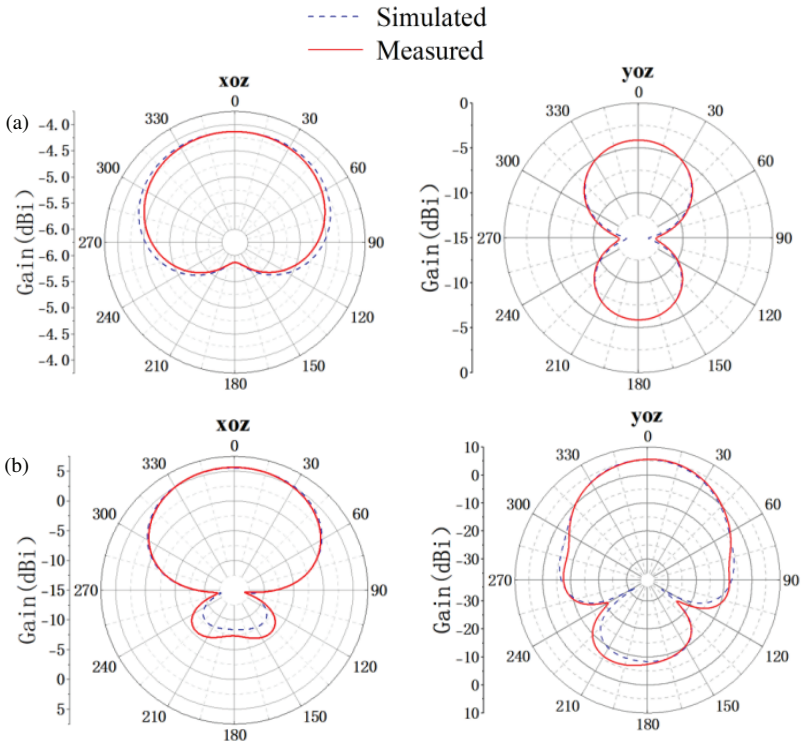

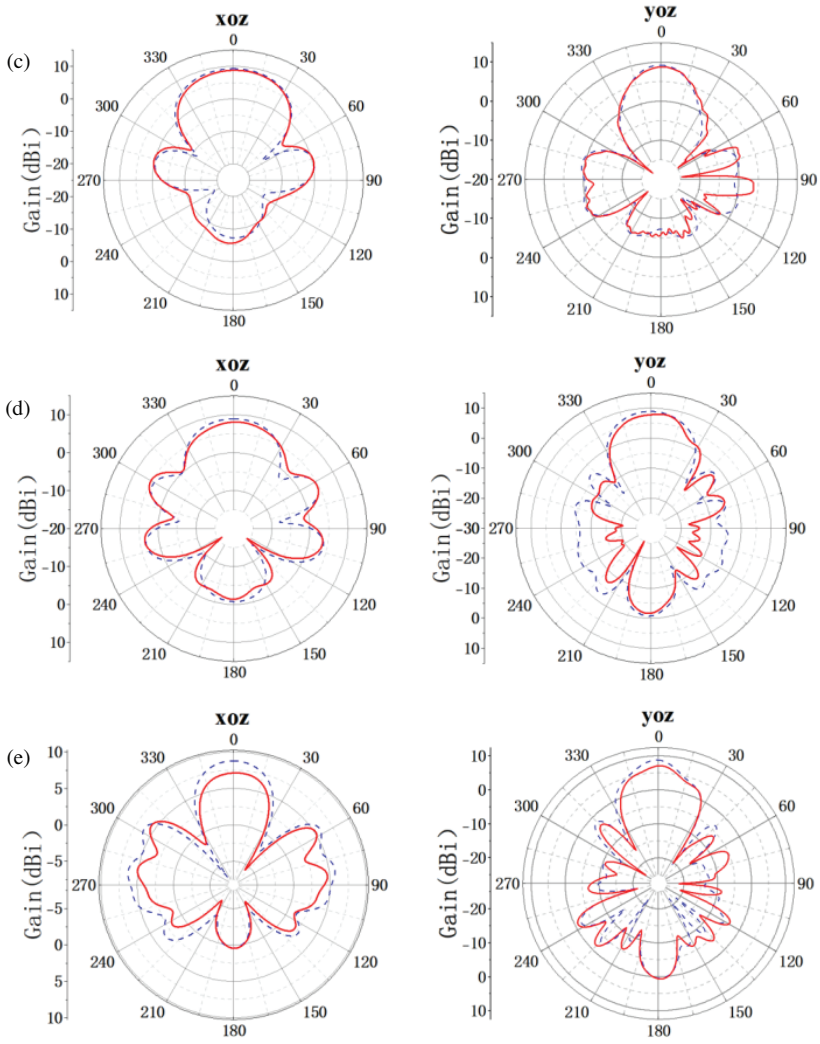

FIGURE 10. Radiation patterns of xoz and yoz planes of the antenna at (a) 0.1 GHz, (b) 0.6 GHz, (c) 1.2 GHz, (d) 1.6 GHz, and (e) 2 GHz.

ing performance deteriorates as the value of R increases. Additionally, an excessively large lumped resistor value reduces the antenna gain. Based on these considerations, $R = 100\,\Omega$ was selected as the optimal value.

4. RESULTS AND DISCUSSION

Based on the simulation results, the physical antenna was fabricated, as shown in Fig. 7. The dimensions of the antenna are $0.137\lambda_L \times 0.133\lambda_L \times 0.05\lambda_L$. The measured and simulated VSWRs are presented in Fig. 8. The results indicate that the measured VSWR closely matches the simulation. Across the operating band from 0.1 GHz to 2 GHz, the VSWR remains below 3.

The measured and simulated gain results of the antenna are shown in Fig. 9. The results indicate that the measured gain is slightly lower than the simulated gain, but it generally aligns with the simulation. The peak gain reaches up to 9 dBi.

Figure 10 presents the simulated and measured radiation patterns of the antenna at frequencies of 100 MHz, 600 MHz, 1200 MHz, 1600 MHz, and 2000 MHz. The results demonstrate that the antenna exhibits good radiation performance across the operating band, with the primary energy radiated in the normal direction.

Table 2 compares the proposed antenna with existing ground-penetrating radar antennas. Although the gain of the proposed antenna is lower than that of [8–11], it achieves a lower cutoff frequency and a more compact size. Additionally, its relative bandwidth is higher than most existing GPR antennas.

5. CONCLUSION

This study enhances the Vivaldi antenna's performance through systematic structural optimization and innovative design. By refining slotline parameters, applying metal loading techniques, and introducing slot structures, the operating bandwidth is effectively expanded. The integration of load resistors further improves impedance matching. The optimized antenna achieves stable operation from 100 MHz to 2000 MHz, covering 20 octaves, while maintaining a compact design. Experimental results show excellent radiation patterns and a maximum gain of 9 dBi. This work provides a valuable approach for designing compact, high-performance broadband antennas.

ACKNOWLEDGEMENT

This project is supported by the Aeronautical Science Foundation of China, Grant No. 20220001081002.

REFERENCES

[1] DuHamel, R. and F. Ore, "Logarithmically periodic antenna designs," in *1958 IRE International Convention Record*, Vol. 6, 139–151, New York, NY, USA, 1966.

[2] Rumsey, V., "Frequency independent antennas," in *1958 IRE International Convention Record*, Vol. 5, 114–118, New York, NY, USA, 1966.

[3] Dyson, J., "The characteristics and design of the conical log-spiral antenna," *IEEE Transactions on Antennas and Propagation*, Vol. 13, No. 4, 488–499, Jul. 1965.

[4] Lee, R. T. and G. S. Smith, "A design study for the basic TEM horn antenna," *IEEE Antennas and Propagation Magazine*, Vol. 46, No. 1, 86–92, Feb. 2004.

[5] Chung, K.-H., S.-H. Pyun, S.-Y. Chung, and J.-H. Choi, "Design of a wideband TEM horn antenna," in *IEEE Antennas and Propagation Society International Symposium. Digest. Held in conjunction with: USNC/CNC/URSI North American Radio Sci. Meeting (Cat. No.03CH37450)*, Vol. 1, 229–232, Jun. 2003.

[6] Wang, S.-F. and Y.-Z. Xie, "Design and optimization of high-power UWB combined antenna based on Klopfenstein impedance taper," *IEEE Transactions on Antennas and Propagation*, Vol. 65, No. 12, 6960–6967, Dec. 2017.

[7] Elmansouri, M. A. and D. S. Filipovic, "Miniaturization of TEM horn using spherical modes engineering," *IEEE Transactions on Antennas and Propagation*, Vol. 64, No. 12, 5064–5073, Dec. 2016.

[8] Lin, S., S. Yu, J.-L. Jiao, and C.-T. Yang, "Simulation and analysis of an ultra-wideband TEM horn antenna with ridge," in *2017 International Symposium on Antennas and Propagation (ISAP)*, 1–2, Phuket, Thailand, 2017.

[9] Wu, J., J. Ma, B. Shi, K.-S. Mo, and L. Peng, "Design of an ultra-wideband low-profile directional bowtie antenna for ground-penetrating radars," in *2024 International Conference on Microwave and Millimeter Wave Technology (ICMMT)*, 1–3, Bejing, China, 2024.

[10] Li, M., R. Birken, N. X. Sun, and M. L. Wang, "Compact slot antenna with low dispersion for ground penetrating radar application," *IEEE Antennas and Wireless Propagation Letters*, Vol. 15, 638–641, 2015.

[11] Guo, L., H. Yang, Q. Zhang, and M. Deng, "A compact antipodal tapered slot antenna with artificial material lens and reflector for GPR applications," *IEEE Access*, Vol. 6, 44 244–44 251, 2018.

[12] Cheng, H., H. Yang, Y. Li, and Y. Chen, "A compact Vivaldi antenna with artificial material lens and sidelobe suppressor for GPR applications," *IEEE Access*, Vol. 8, 64 056–64 063, 2020.

[13] Lv, H., Q. Huang, J. Hou, and J. Liu, "Wideband dual-polarized Vivaldi antenna with gain enhancement," *Applied Computational Electromagnetics Society Journal (ACES)*, Vol. 33, No. 9, 990–996, 2018.

[14] Karmakar, A., A. Bhattacharjee, A. Saha, and A. Bhawal, "Design of a fractal inspired antipodal Vivaldi antenna with enhanced radiation characteristics for wideband applications," *IET Microwaves, Antennas & Propagation*, Vol. 13, No. 7, 892–897, 2019.